Molecular Beam Scattering Experiments on Benzene−Rare Gas Systems: Probing the Potential Energy Surfaces for the C_6H_6−He, −Ne, and −Ar Dimers†

D. Cappelletti*

INFM and Dipartimento di Ingegneria Civile ed Ambientale, Università di Perugia, 06125, Perugia, Italy

M. Bartolomei, F. Pirani, and V. Aquilanti

INFM and Dipartimento di Chimica, Università di Perugia, 06123, Perugia, Italy

Received: January 28, 2002

Molecular beam scattering measurements of total cross sections have been performed at a sufficiently low energy in the thermal range and at an angular resolution high enough to permit for the first time the observation of the "glory" interference effect in collisions of a benzene molecule with He, Ne, and Ar. Information on range, strength, and anisotropy of the interaction in the C_6H_6− rare gas dimers has been obtained from the analysis of the energy dependence of the total cross sections. In benzene−He, −Ne, and −Ar dimers bond energies are 0.98, 1.95, and 4.20 kJ/mol, respectively, for the most stable geometry, in all cases an out-of-plane configuration with the rare gas atom located on the 6-fold symmetry axis of benzene, at distances of 0.323, 0.331, and 0.359 nm, respectively. The results of the present investigation show that well depths for all three systems decrease by a factor 2 or 5 and corresponding distances increase by 40% or 70% for planar rare gas approaches respectively perpendicular to a C−C bond or collinear to a C−H bond (estimated uncertainties of 10% for bond energies and 3% for bond lengths). These experimental findings provide a crucial test of correlation formulas recently proposed (*Chem. Phys. Lett.* **2001**, *350*, 286−296) to estimate van der Waals minimum well depths and distances at selected approach geometries of rare gases on hydrocarbons.

I. Introduction

The characterization of binding effects in aggregates of increasing complexity represents a crucial objective for investigations of microscopic and macroscopic properties of the matter. The benzene−rare gas complexes, interacting via pure van der Waals forces, have received particular attention, being considered as prototype systems both for the solvation of planar molecules (one or more atoms attached to the substrate) and for the interaction of a spherical particle with an aromatic π-ring. And the role played by molecular interactions involving aromatic π-ring complexes is of great relevance in chemistry, molecular physics, and biology.

Several *spectroscopic* investigations,[1−17] involving various techniques and probing different wavelength regions, have been carried out on benzene−rare gas clusters in order to determine their structure and their intermolecular dynamics. Spectroscopic experiments provide valuable information on the geometry, equilibrium distance, and force constants of the bending and stretching modes for the more stable configuration of the investigated system. The main finding of such studies is that the benzene−rare gas dimer tends to assume the shape of a symmetric top complex with the rare gas atom located on the 6-fold symmetry axis of benzene (out-of-plane configuration). For some systems the spectroscopic studies were also able to provide quantitative estimates on the binding energy in the most stable configuration: for example for benzene−Ar an upper limit of 3.78 kJ/mol has been recently proposed for the dissociation energy.[15]

It is the purpose of this paper to show that information on the range and strength of the interaction for different geometries of the complex can be obtained from *scattering* experiments and specifically from the measurements of collision cross sections and their velocity dependence on thermal energies. However these experiments require high angular resolution to measure the "true" quantum total cross section and it is particular demanding to characterize the quantum interference structure, which is very sensitive to the interaction anisotropy and whose effect on the observables strongly depends on the experimental conditions. The only previous scattering study reported in the literature on benzene−He[18] yielded an unrealistic anisotropic potential because of the broad thermal distribution of benzene in the beam source.

The target of the present study is the measurement, as a function of the collision energy, of the "glory" structure, an oscillatory pattern superimposed on the smooth component of the velocity dependence of the total cross sections.[19] As is well-known, the smooth component is affected by the long-range attraction, while the glory structure, arising from a quantum interference due to forward scattering (near zero deflection angle), depends on the properties of the well in the neighborhood of the minimum in the intermolecular potential.[20]

The effect of the rotational temperature on the glory structure was initially ascertained experimentally several years ago[21] for collisions of O_2 on Kr. The scattering experiment showed that the glory ondulatory pattern exhibits a quenching of the amplitude and a shifting of the extrema location when measured with rotationally "cold" O_2 molecules. This is a a manifestation of the interaction anisotropy and so this effect disappears when

† Part of the special issue "R. Stephen Berry Festschrift".

10.1021/jp0202486 CCC: $22.00
Published on Web 09/26/2002

rotationally "hot" molecules are employed, because the rapidly rotating molecules approach the collisional behavior of an effective spherical atom. Here, "cold" and "hot" are clearly attributes coming from comparison of rotational energy and collisional energy. Indeed a crucial parameter to be considered, in planning and analyzing scattering experiments, is the ratio between the collision time, t_{coll}, and the typical time, t_{av}, associated with the molecular rotation period τ, which is required to average the interaction among limiting configurations of the system. The collision time varies with the collision velocity, scaled over the range of the potential, while the averaging time of molecular rotations depends on the temperature and on the internal motion modes of relevance. When the collision velocity is high the molecular anisotropy strongly influences elastic and inelastic events and sudden models can be employed for calculations of the dynamics. In contrast when the velocity is low the role of the anisotropy becomes negligible and collisions are mainly driven by the average component of the interaction.

The characterization of the fundamental features of clusters involving benzene is also one of the challenging tasks of computational chemistry. Several *ab initio*, semiempirical and empirical methods have been developed to describe the interactions in the benzene−rare gas systems,[22−25] providing a reliable description of the potential energy surface (PES) in the neighborhood of the most stable geometry. Here the interaction energy can assume values on the order of few kilojoules per mole. However, information on the full topography of the PES is lacking: in particular, details of the interaction, when the rare gas atom approaches the benzene molecule along its molecular plane (in-plane configurations), are known with much less accuracy (the bond energy is expected to be much lower with respect to that of the most stable configuration). It should be noted that even the most recent and accurate calculations[25] for the benzene−argon dimer overestimate the binding energy in the most stable configuration outside the experimental uncertainty.[15] It should be also stressed that the full PES, and in particular the in-plane interaction, plays a crucial role in the collision dynamics of benzene molecules, driving elastic, inelastic, and reactive events.

Several efforts have been addressed in our group to find a proper description of the main interaction components, in terms of fundamental physical properties of the interacting partners. Our aim has been the search of a procedure of general validity, useful to describe systems of increasing complexity covering a range of interaction energies varying from a few to several kilojoules per mole. Recently we have developed a new empirical method[26] suitable to evaluate bond energy, equilibrium distance, and long-range attraction in rare gas atom−hydrocarbon molecule systems. This method, applicable to any geometry of the complex, employs correlation formulas which provide these basic interaction features in terms of atomic and molecular bond polarizabilities. They represent an extension of formulas previously introduced[27] to represent the van der Waals interaction in atom−atom systems. The results of this procedure can be inserted in a potential model to predict the features of the PES at any geometry of the complex. See also related work on ionic interactions[28,29] and on open shell−closed shell interactions.[30]

The present paper reports on a new set of collisional experiments, carried out using rare gas atom beams, scattered on benzene molecules, to measure the dependence of the total cross section on the beam velocity. This technique has been applied for more than two decades for the measurements of intermolecular forces, the most recent examples being[31] for

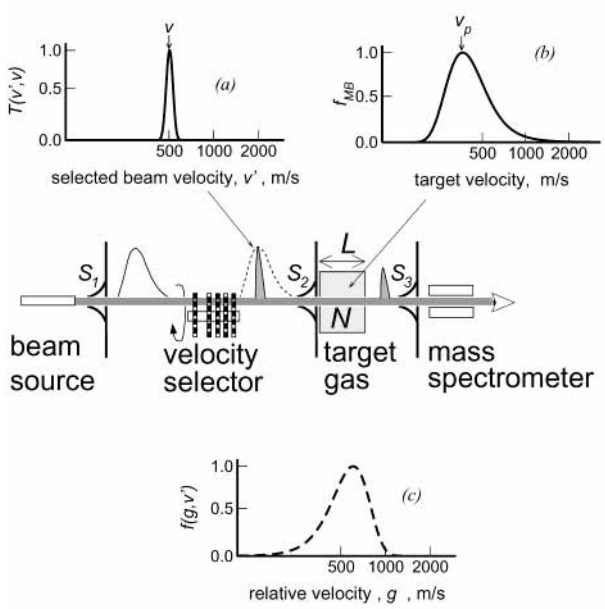

Figure 1. Sketch of the experimental apparatus. (a) Velocity distribution $T(v', v)$ of a projectile beam as transmitted by the velocity selector. (b) Boltzmann velocity distribution f_{MB} of the target benzene molecules kept at room temperature. (c) Relative velocity distribution $f(g, v')$ as obtained by combining the peak velocity of the beam in (a) and the thermal motion of the target in (b).

atom−atom,[32] for atom−molecule, and[33,34] for molecule−molecule systems. The choice of suitable experimental conditions, determining both the investigated collision energy range and the rotational temperature of molecules, allowed us to resolve for the first time the glory structure for the investigated systems. As will be discussed later such an interference structure appears to be strongly sensitive to the in-plane configuration interactions. Therefore measured data for benzene−rare gas systems permit the characterization of the intermolecular potentials and represent a test of the accuracy of the proposed correlation formulas for the estimate of the relevant features of the interactions of rare gases with hydrocarbons.[26]

Section II illustrates some details of the experimental apparatus and describes the procedure adopted to measure interference effects in the quantum cross section. Cross section results for C_6H_6−He, −Ne, and −Ar systems are reported in section III. A comparison among observations and predictions is shown in section IV, while a discussion and conclusions follow in section V.

II. The Apparatus

The experimental apparatus employed for measurements described in this paper consists of a set of differentially pumped vacuum chambers connected by slits for molecular beam collimation. The molecular beam emerges through a ∼1-mm nozzle diameter from a source which can operate under effusive or moderately supersonic conditions. After velocity selection, the beam crosses a scattering chamber, which can be filled with the target gas by an automated procedure. The on-line beam intensity is detected, after the scattering region, by an electron bombardment ionizer followed by a quadrupole mass spectrometer. A sketch of the apparatus is shown in the upper part of Figure 1, while critical dimensions and various operating conditions are reported in Table 1. The apparatus is basically the same as previously employed in other scattering studies,[31,33,34] but recently, the distance between the detector and the scattering chamber has been increased from 100 to 150 cm to improve the angular resolution conditions.

TABLE 1: Critical Dimensions of the Apparatus and Typical Operating Conditions

molecular beam defining slits	
S_1	1.2 mm
S_2	0.7 mm
S_3	1.2 mm
S_2-S_3 distance	∼150 cm
molecular beam source	
nozzle diameter	1.0 mm
stagnation pressure	3−30 mbar
nozzle temperature	90−570 K
scattering chamber	
temperature	300 K
target pressure range	$10^{-2}-10^{-3}$ mbar
target density, N	$10^{15}-10^{14}$ molec/cm^3
scattering path length, L	∼7 cm

The measurement of the beam attenuation I/I_0 (where I and I_0 represent the beam intensity with and without target gas in the scattering chamber) at selected beam velocity, v, permits the determination of the total (elastic + inelastic) integral cross section $Q(v)$ in the laboratory frame:

$$Q(v) = -\frac{1}{NL}\log\frac{I}{I_0}$$

where N is the target gas density and L the scattering region length (Table 1). The experimental $Q(v)$ is related to the center-of-mass cross section $Q^{CM}(g)$, which is a function of the relative velocity g, through the following relationship:

$$Q(v) = R(v)\int_0^\infty \mathrm{d}v'\, T(v',v)\int_0^\infty \mathrm{d}g\, Q^{CM}(g)\, f(g,v')$$

where $R(v)$ is an apparatus dependent factor which limits the value of the measured cross section because of the finite angular resolution of the experiment, $T(v', v)$ represents the transmission function of the velocity selector, for which the peak velocity is v and the full width at half-maximum is ∼5%, and $f(g, v')$ is the relative velocity distribution function to be defined below. The $R(v)$ function is defined[35] in terms of the ratio between the angular resolution of the apparatus and the limiting angle of the experiment (see also ref 36). It depends on dimensions of and distance between the collimation slits S_2 and S_3 (see Figure 1 and Table 1), on the mass and velocity of the projectile, and on the value of the cross section. Here $T(v', v)$ is approximated with a triangular function[37] and $f(g, v')$, which arises from combining the motion in the forward direction of a velocity-selected projectile with the random motion of a target gas at thermal equilibrium, takes the form[37]

$$f(g,v') = \frac{1}{\pi^{1/2}v_p}\left(\frac{g}{v'}\right)^2\left\{\exp\left[-\left(\frac{v'-g}{v_p}\right)^2\right] - \exp\left[-\left(\frac{v'+g}{v_p}\right)^2\right]\right\}$$

where v_p is the most probable velocity of the target particles at the scattering chamber temperature.

For the experiments described in this paper, rare gas atoms have been employed as projectiles in the velocity-selected beam, while benzene molecules, kept at room temperature in the scattering chamber, represent the target. The lowest panel of Figure 1 shows the behavior of $f(g, v')$ for the selected projectile velocity $v' = v = 500$ m/s (a in Figure 1), at the v_p value corresponding to the random motion of the benzene target molecules having a Boltzmann distribution f_{MB} at room temperature (b in Figure 1). The effect of $f(g, v')$ (c in Figure 1) is seen to be of great relevance, since it directly influences the observation of the interference pattern in the laboratory frame.

TABLE 2: Rotational Period τ for Rotational Motion around the C_{6v} and C_{2v} Axes of the Benzene Molecule at Two Different Rotational Temperatures[a]

	$T_{rot} = 300$ K	$T_{rot} = 25$ K[b]
C_{2v}	$\tau = 3.7\times10^{-12}$	$\tau = 1.3\times10^{-11}$
	$t_{av}\sim 1\times10^{-12}$	$t_{av}\sim 3\times10^{-12}$
C_{6v}	$\tau = 5.6\times10^{-12}$	$\tau = 1.8\times10^{-11}$
	$t_{av}\sim 5\times10^{-13}$	$t_{av}\sim 1.5\times10^{-12}$

[a] t_{av} is the time needed to obtain an average of the interaction between two limiting configurations. All times are in seconds. [b] This case describes the behavior of rotationally cold benzene molecules flying in supersonic beams and colliding with rare gas atom targets.[38]

TABLE 3: Collisional Time, t_{coll}, at Three Different Beam Velocities, v, Are Reported Together with the Dynamical Regimes of the Benzene Molecules under Various Conditions

		benzene dynamical regimes	
v, m/s	t_{coll}, s	$T_{rot} = 300$ K	$T_{rot} = 25$ K[a]
500	$\sim2\times10^{-12}$	sphere	disk
1000	$\sim1\times10^{-12}$	sphere/disk	disk/hexagon
2000	$\sim5\times10^{-13}$	disk	hexagon

[a] This case describes the behavior of rotationally cold benzene molecules flying in supersonic beams and colliding with rare gas atom targets.[38]

The experimental configuration adopted here is complementary with the one where benzene is the projectile and its scattering by rare gas targets served us in studying its alignment in seeded beams emerging from a supersonic expansion.[38] The choice of the present alternative configuration has been motivated by the following considerations. The first one refers to the necessity of minimizing the effect of the angular resolution, as represented by the $R(v)$ function. Under the present experimental conditions, the use of the lighter rare gases He, Ne, and Ar as a projectile, instead of the heavier benzene molecule, is crucial to observe in the laboratory frame the quantum interference pattern (the "glory" effect), whose amplitudes are typically of the order of 10% of the value of the cross section. Using Ar as a projectile, the maximum expected correction is of the order of 1% ($R(v) \sim 0.99$) at the highest explored beam velocities ($v \geq 1500$ m/s). For an experiment with benzene in the beam scattered on Ar, such correction would increase up to ∼20% ($R(v) \sim 0.80$) in the same velocity range. A second important issue is connected with the possibility of cluster formation in the expansion region, even if moderately supersonic beams of benzene were employed. By contrast, in the scattering chamber kept at a temperature of ∼300 K and at a pressure of $\sim10^{-2}$ mbar the percentage of benzene dimers is ≪1%, this can be calculated by a semiclassical procedure[39] taking into account existing information on the bond energy of the dimer.[40] Furthermore, under the above conditions the benzene molecules are randomly oriented, they show an average rotational period sufficiently short to induce a more or less complete averaging of the interaction anisotropy during each collision, and the probability of inelastic events is reduced. The various experimental conditions pertinent to the present study can be identified by examining the average rotational and collisional times reported in Tables 2 and 3.

Finally, a rare gas beam source can operate in wider temperature and pressure ranges with respect to a benzene beam source, covering a larger collision energy spectrum. A difficulty

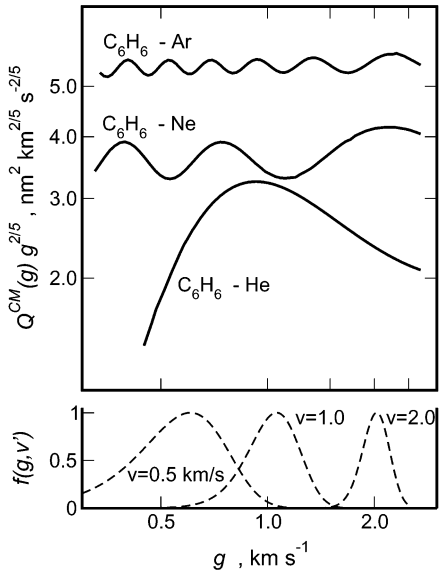

Figure 2. Upper panel: total cross sections $Q^{CM}(g)$ in the center-of-mass reference frame as calculated for the C_6H_6-He, $-$Ne, and $-$Ar systems with the spherical interaction component obtained in ref 26. Lower panel: relative velocity distributions $f(g, v')$ corresponding to three specific beam velocities and assuming the target at room temperature (see text and Figure 1).

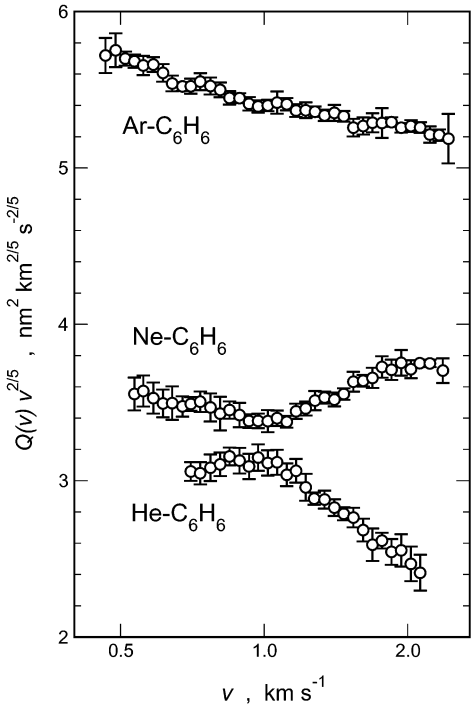

Figure 3. Total cross section $Q(v)$ for scattering of a rare gas (He, Ne, and Ar) beam by benzene target molecules measured as a function of the beam velocity v. Experiments do not provide an absolute scale. The one given comes from the comparison with calculations (see Figures 7−9).

is, however, connected with the accurate calibration of the benzene pressure in the scattering chamber.

To choose the best operating conditions, a simulation of the experiment has been carried out, calculating the integral cross sections in the center-of-mass system using the spherical interaction[26] (see also below) which represents the main interaction component. The calculated cross sections $Q^{CM}(g)$, for He, Ne, and Ar colliding with benzene, are reported in Figure 2 as a function of the relative velocity g and plotted as $Q^{CM}(g)g^{2/5}$ (this is the usual procedure, which emphasizes the glory pattern). In the lower panel of the Figure 2 are also shown the relative velocity distribution functions $f(g, v')$, corresponding to three specific projectile beam velocities $v = 500$, 1000, and 2000 m/s and considering the benzene target at room temperature.

The comparison between the period of the glory structure and the width of the $f(g, v')$ function (specifically, its full width at half-maximum) suggests the proper range of beam velocities where the quantum interference pattern can be observed in a real experiment. In the case of Ar the width of the $f(g, v')$ function becomes smaller than the period of the glory pattern only at beam velocities $v \geq 1500$ m/s, and therefore the quantum interference effects are measurable only in such a v range. In the case of Ne such effects are observable for $v \geq 500$ m/s.

For scattering of He by atoms or simple molecule, glory structures have never been observed before, because the van der Waals interactions, driving collision complexes, are too weak to provide glory interference effects observable only at subthermal collision energies.

In He−benzene, the relatively strong van der Waals interaction, associated with the large polarizability of the benzene molecule, produces an ample and low-frequency glory pattern observable in the intermediate velocity range (∼1000 m/s), while the most probable velocity of a thermal effusive He beam is ∼1400 m/s. The simulation of Figure 2 suggests that a successful experiment can be carried out using a cold source of He atom beam. This is the reason the source nozzle was cooled to liquid air temperature (∼90 K).

III. Experimental Results

Integral cross sections $Q(v)$, measured as a function of the selected beam velocity v for the three investigated systems, are reported in Figure 3. Glory oscillations have been clearly resolved in He$-C_6H_6$ and Ne$-C_6H_6$ collisions, while in the case of Ar$-C_6H_6$ they appear much less evident. These results are consistent with the simulation discussed in the previous section. A preliminary analysis was performed by the comparison of the integral cross sections measured here with those of the previously investigated atom−atom systems, He−Xe,[41] Ne−Xe,[42] and Ar−Xe.[43] The similarity of frequency and location of the glory extrema suggests that the strength of the interactions, in the intermediate intermolecular distance region mainly probed by these experiments and involving the potential wells, falls in the range of the corresponding rare gas complexes with xenon.[41−43]

Since under the present experimental conditions the collisions of rare gases with benzene molecules are mainly driven by an effective spherically averaged interaction (as outlined in section I and further amplified in section IV), being the component of the interaction mostly determined by in-plane configurations, the scattering results reported in this paper provide direct information on the planar geometry interactions of the dimers.

Therefore the present experiments on the benzene−rare gas systems are complementary to spectroscopic investigations, which are sensitive to the most stable out-of-plane configuration, and a combined analysis provides a full picture of the potential energy surfaces for such complexes.

IV. Data Analysis

The present investigation exploits the calculation, within different dynamical regimes, of the center-of-mass cross sections $Q^{CM}(g)$, which directly depend, as anticipated in section II and more extensively discussed below, on characteristic features of

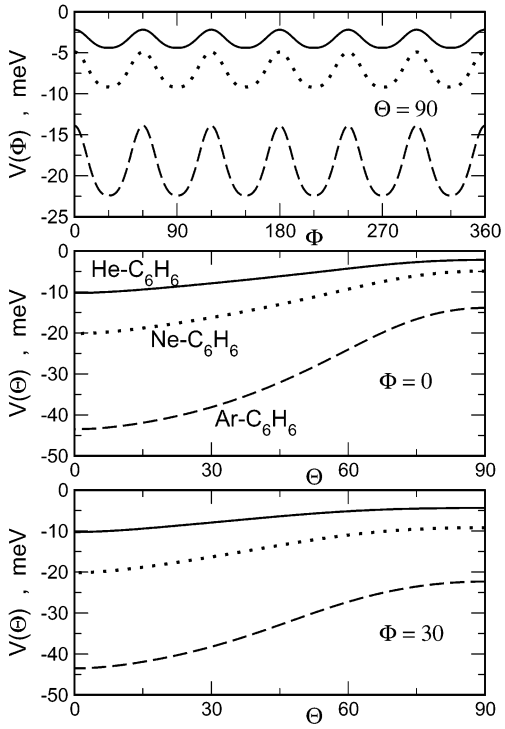

Figure 4. Angular dependence of the interaction energy at the equilibrium distance for He− (continuous lines), Ne− (dotted lines), and Ar−benzene (dashed lines) systems. Upper panel: in plane ($\Theta = 0$). Central panel: out of plane ($\Phi = 0$). Lower panel: out of plane ($\Phi = 30$) (see Figure 5 for the adopted nomenclature).

the potential energy surface (PES) driving the collisions. For a comparison with the experimental data, calculated cross sections are convoluted in the laboratory frame as described in section II. The main features of the PES in the C_6H_6−He, −Ne, and −Ar complexes have been anticipated by using new correlation formulas[26] based on the assumption that a polyatomic molecule, interacting with a closed-shell atom, behaves as a cluster of diatomic molecules each of them corresponding to a particular bond of the molecule. This is equivalent to treating the interaction as determined by a repulsion due to an effective size of the molecule and an attraction arising from different dispersion centers distributed on the molecule. The method provides, by proper correlation formulas given in terms of atomic and molecular bond polarizabilities, the relevant coefficients for the long-range expansion of the potential attraction, the equilibrium distance R_m, and the depth of the van der Waals well ϵ for a given geometry of the complex. Such an approach represents an extension of the methodology successfully used to describe the interaction in a variety of atom−atom systems.[27] Figure 4 shows the angular dependence of the PES, at R_m, for the benzene−rare gas systems investigated in this paper. The adopted nomenclature is introduced in Figure 5. Corresponding cuts of the PES's, obtained by interpolating the results of correlation formulas with the parametrization given in the Appendix, are plotted in Figure 6. Tables 4−6 report the well depths ϵ and R_m values and other relevant details of the intermolecular potential energy functions, which have been used for the calculations of the cross section $Q^{CM}(g)$, for the spherical component of the interaction, V_0, and for three selected approach geometries of the complex.

In the present analysis we have found it appropriate to distinguish among different dynamical regimes for scattering, each one selectively governed by specific features of the PES. Such regimes (see Figure 5) emerge as a function of the beam velocity and can be classified by comparing the collision time t_{coll}, namely, the time needed to traverse a distance $\sim 1.0 \times 10^{-9}$ m (corresponding to twice the glory impact parameter[44]), with the typical time t_{av} required to average between limiting configurations of the collision complex. The latter is related to the average rotational period τ and therefore to the rotational temperature of benzene.

The estimated times, reported in Tables 2 and 3, indicate that at low collisional velocities benzene molecules at room temperature are seen, by the colliding atom, as rotating sufficiently fast to be considered as spheres (limiting case 1 in Figure 5). Therefore at low velocities a dynamical regime must apply where it is proper to consider the scattering to be elastic and guided by the spherical component of the interaction. In the high velocity range a second collisional regime sets in, where benzene behaves like a disk-shaped target (rapidly rotating) randomly oriented (described as a combination of frisbee and flywheel configurations, cases 2 and 3 in Figure 5).

To emphasize differences in the scattering behavior of molecules confined in the various regimes, we have calculated, for all investigated systems, cross sections in the laboratory frame at fixed geometry of the collision complex, specifically for an out-of-plane (A in Figure 5), a vertex-in-plane (B in Figure 5), and a side-in-plane approach (C in Figure 5). Results

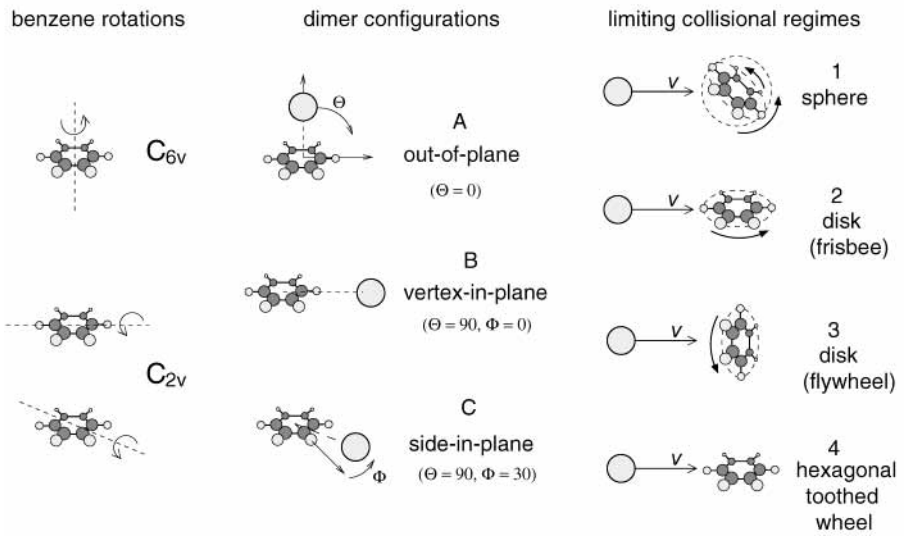

Figure 5. Benzene−rare gas complex: relevant nomenclature.

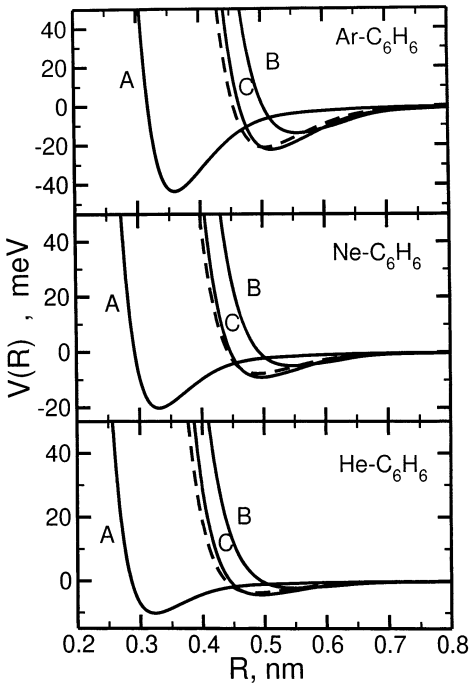

Figure 6. Relevant cuts of the potential energy surfaces: full curves refer to dimer configurations described in Figure 5 and the dashed ones represent the spherical component V_0.

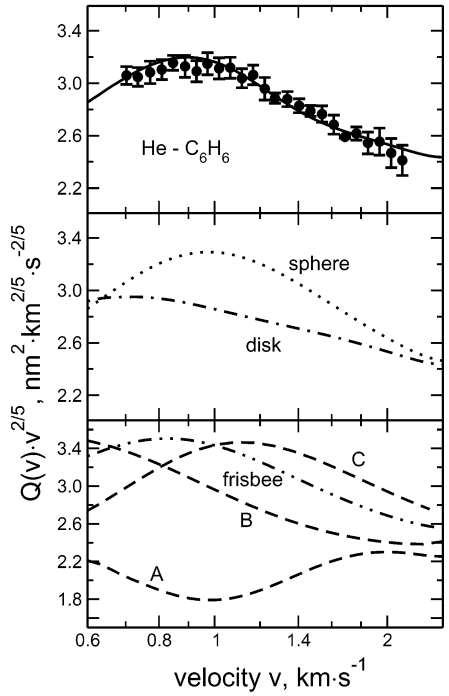

Figure 7. Comparison in the laboratory frame between experimental total cross section data, measured for He projectiles scattered by benzene targets, and calculations performed with the proposed interaction (see Table 4 and also ref 26) and considering the dynamical regimes discussed in the text. Lower panel: dashed curves represent predicted cross sections for fixed geometries of the collisional complex (A, B, and C in Figure 5), while the dot−dashed curve is calculated assuming benzene as a disk (rapidly rotating) in the frisbee configuration (case 2 in Figure 5). Middle panel: the dotted curve is calculated taking benzene as a spherical particle, while the dot−dashed curve represents the behavior of a randomly oriented disk (67% of frisbee and 33% of flywheel). Upper panel: Experimental data (full circles) and calculations (continuous curve) obtained assuming benzene as a spherical particle at low velocities and as a disk-shaped target randomly oriented at high velocities (see text).

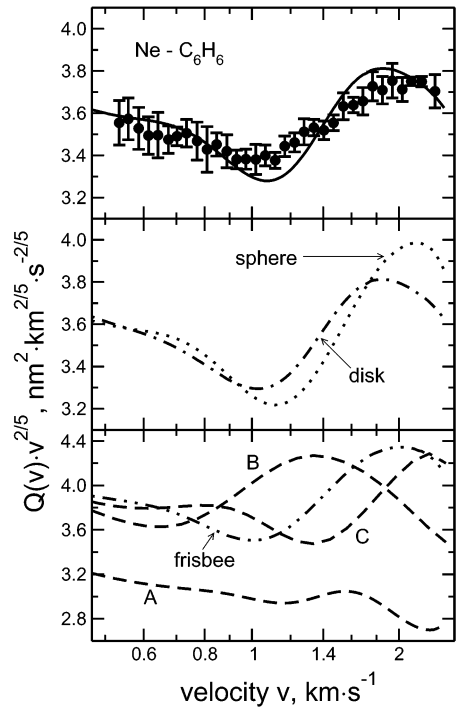

Figure 8. As in Figure 7, for Ne projectiles scattered by benzene targets. Employed potential parameters are in Table 5 (see also the text).

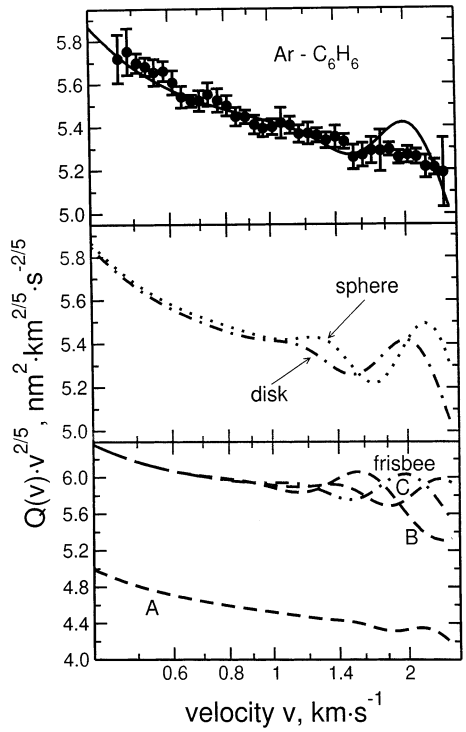

Figure 9. As in Figure 7, for Ar projectiles scattered by benzene targets. Employed potential parameters are in Table 6 (see also the text).

are plotted in the lowest panels of Figures 7−9. In the same figures calculated data, corresponding to a rotational averaging of the benzene interaction anisotropy, are also plotted. They illustrate the predicted behavior of a rapidly rotating frisbee (lowest panels), obtained by averaging the in-plane anisotropy of benzene, so that the interaction is defined as the average of those corresponding to the configurations B and C and of a spherical molecule (intermediate panels), whose interaction

TABLE 4: Potential Parameters (See Ref 26 and the Appendix) Defining the Spherical Component V_0 and Some Cuts (A, B, and C, See Figure 5) of the Potential Energy Surface for the C_6H_6−He System

	V_0	A	B	C
ϵ, meV[a]	3.8	10.2	4.4	2.2
R_m, nm	0.485	0.323	0.493	0.549
b	7	6	7	7
C_6, meV nm^6	3.53×10^{-2}	3.00×10^{-2}	3.80×10^{-2}	3.80×10^{-2}
b	5.78	−10	12	12
x_1	1.12	1.15	1.10	1.10
x_2	1.48	1.75	1.38	1.30

[a] 1 meV = 9.648×10^{-2} kJ mol^{-1}.

TABLE 5: Potential Parameters (See Ref 26 and the Appendix) Defining the Spherical Component V_0 and Some Cuts (A, B, and C, See Figure 5) of the Potential Energy Surface for the C_6H_6−Ne System

	V_0	A	B	C
ϵ, meV[a]	7.76	20.2	9.1	4.9
R_m, nm	0.491	0.331	0.496	0.547
b	7	6	7	7
C_6, meV nm^6	6.90×10^{-2}	6.35×10^{-2}	7.68×10^{-2}	7.68×10^{-2}
b	5.57	−10	12	12
x_1	1.12	1.15	1.10	1.10
x_2	1.48	1.75	1.38	1.30

[a] 1 meV = 9.648×10^{-2} kJ mol^{-1}.

corresponds to the full average of the intermolecular potential on the possible relative orientations (see also Figure 6). It is clear that both slowly and rapidly rotating flywheels (configuration A and collision regime 3 in Figure 5) exhibit the same total cross sections because they interact in the same way. However, marked differences are expected in the behavior of rapidly and slowly rotating frisbees, the latter being more sensitive to the in-plane anisotropy of benzene. The effect can be depicted as that due to an "hexagonal toothed wheel" (limiting case 4 in Figure 5), and cross sections are correspondingly given as averages of those related to B and C configurations. This procedure leads even in the center of mass system to a pronounced quenching of the glory pattern.

In the present analysis, calculated cross sections have been defined within the spherical molecule behavior at $v \leq 0.8$ km/s and as a combination of fast rotating frisbee and flywheel (respectively 67% and 33% according to their weight in the representation of a randomly oriented disk) for $v \geq 1.6$ km/s. The switch between these two dynamical regimes at intermediate v was carried out by a weighted sum (the weights depending on the velocity) of cross sections calculated for the two limiting cases which are shown in the intermediate panels of Figures 7−9. Calculated cross sections are compared with the experimental data in the upper panel of Figures 7−9.

V. Discussion and Conclusions

Potential parameters of Tables 4−6 provide calculated cross sections in agreement with the experimental data. In particular, the measured glory extrema positions and frequency are well described in all cases (see Figures 7−9). The glory amplitude is satisfactorily reproduced for C_6H_6−He and C_6H_6−Ne, while a partial quenching is exhibited by the glory pattern of the C_6H_6−Ar system. This quenching is a manifestation of the effect of the interaction anisotropy on a high-frequency interference oscillation, such as that involved in the C_6H_6−Ar system (see Figure 2). Note also that at the largest explored beam velocities ($v \sim 2.0$ km/s) the colliding system falls in a dynamical regime where the benzene target shows an intermediate behavior

TABLE 6: Potential Parameters (See Ref 26 and the Appendix) Defining the Spherical Component V_0 and Some Cuts (A, B, and C, See Figure 5) of the Potential Energy Surface for the C_6H_6−Ar System[a]

	V_0	A	B	C
ϵ, meV[b]	21.2	43.5	22.3 (26.9)	13.9 (15.3)
R_m, nm	0.505	0.359	0.516 (0.503)	0.558 (0.552)
b	7	6	7	7
C_6 (meV nm^6)	2.17×10^{-1}	1.71×10^{-1}	2.56×10^{-1}	2.56×10^{-1}
b	11	−10	18	18
x_1	1.12	1.15	1.10	1.10
x_2	1.48	1.75	1.38	1.30

[a] Calculated results from ref 25 are in parentheses. [b] 1 meV = 9.648×10^{-2} kJ mol^{-1}.

TABLE 7: Interaction Features for Benzene−Rare Gas Systems in the Out-of-Plane Configuration (Case A in Figure 5)

	ϵ, meV	R_m, nm	
C_6H_6−He	10.2	0.323	ref 26
		0.317	exptl[1]
	8.4		calcd[22]
C_6H_6−Ne	20.2	0.331	ref 26
	18.7[a]	0.330	exptl[8]
	19.8	0.332	calcd[23]
C_6H_6−Ar	43.5	0.359	ref 26
	<49.4[a]	0.358	exptl[7]
	50.5[a]	0.350	exptl[8]
	<46.4[a]		exptl[15]
	47.9[a]	0.355	calcd[25]

[a] Calculated zero point energies were added to the experimental dissociation energies.[7,22,23]

between that of a randomly oriented disk and a randomly oriented flat hexagon: the latter is represented as a combination of a toothed wheel (67%) and a flywheel (33%) (see limiting cases 3 and 4 in Figure 5). Under such conditions, a more pronounced quenching of the calculated glory amplitude in the C_6H_6–Ar system is expected.

The very good agreement illustrated in Figures 7−9 represents a crucial test both of the reliability of the potential parameters used and of the dynamical regimes for scattering employed in this analysis. In particular, present scattering experiments are mainly affected by in-plane interactions and they are well described by the potential parameters of Tables 4−6. For C_6H_6−Ar the interactions used are close to the results of most recent ab initio calculations (see Table 6). A detailed analysis of present experimental findings indicates also that the uncertainties associated with the relevant potential parameters are ±10% for ϵ and ±3% for R_m. Moreover, well depth and equilibrium distance in the out-of-plane configuration, obtained in ref 26, agree very well for all systems, as shown in Table 7, with spectroscopic determinations and are in the range of more recent theoretical calculations. Therefore we can conclude that predicted potential features[26] are accurate in all limiting configurations for the cases of interest. The results of this work open new perspectives in the study of collision dynamics in benzene−rare gas systems. For instance the availability of an accurate PES is basic to properly describe elastic and inelastic single collision events and to further model multicollisional processes generating alignment of the plane of molecular rotation in supersonic expansions. Moreover, such knowledge is also crucial in the tuning of the scattering as a probe of the degree of benzene alignment and of its dependence on the velocity. Such a study involves measurement of anisotropy effects in the cross sections and results are already available (for a preliminary analysis see ref 38).

In conclusion present experiments provide direct information on some relevant features of the PES's in benzene−rare gas systems and represent an important reliability test of the predictions of the empirical method[26] recently developed in our laboratory and shown to be able to anticipate the characteristic parameters of the hydrocarbon−closed shell atom intermolecular potentials.

Acknowledgment. This research has been supported by the Italian MIUR (Ministero dell'Istruzione, dell'Università e della Ricerca), by the ENEA (Ente per le Nuove Tecnologie, l'Energia e l'Ambiente) and ASI (Agenzia Spaziale Italiana), and by the EU through the Human Potential Research Networks "Generation, Stability and Reaction Dynamics of Multiply Charged Ions in the Gas Phase" (contract no. HPRN-CT-2000-00027) and "Theoretical Studies of Electronic and Dynamical Processes in Molecules and Clusters" (contract no. HPRN-CT-1999-00005).

Appendix A. Parametrization of the Potential Energy Surfaces

The spherical interaction component V_0 (obtained by averaging over all possible molecular orientations) and some relevant cuts of the potential energy surfaces, used for the analysis of the experimental data (see text), have been represented by a standard procedure for van der Waals forces. Each potential energy curve $V(R)$ has been described by the following MSV (Morse-switching van der Waals) parametrization, scaled for location R_m and depth ϵ of the potential well. Defining

$$x = \frac{R}{R_m} \tag{5.1}$$

we have

(i) Morse for $x \leq x_1$

$$\frac{V(R)}{\epsilon} = \exp[-2\beta(x-1)] - 2\exp[-\beta(x-1)] = M(x) \tag{5.2}$$

(ii) switching from Morse to van der Waals for $x_1 < x < x_2$

$$\frac{V(R)}{\epsilon} = S(x)\,M(x) + [1 - S(x)]W(x) \tag{5.3}$$

where $M(x)$ is as in eq 5.2 and the "switching" function is

$$S(x) = \frac{1}{2}\left[\cos\frac{\pi(x-x_1)}{(x_2-x_1)} + 1\right] \tag{5.4}$$

(iii) van der Waals for $x \geq x_2$

$$\frac{V(R)}{\epsilon} = -\frac{C_6}{\epsilon R_m{}^6 x^6}\left(1 + \frac{b}{R_m{}^2 x^2}\right) = W(x) \tag{5.5}$$

where C_6 is a phenomenological constant defining the induced dipole-induced dipole interaction which varies as R^{-6}. The b parameter differentiates the asymptotic attraction from a pure R^{-6} behavior. Note that for V_0 and for the in-plane configurations, b must assume positive values in order to include the contribution of higher order interaction and to represent the effect of the different distance of the various molecular bonds from the probe atom. For the out-of-plane configuration, b must be negative since the long-range potential tends to the atom−graphite plane attraction, which changes as R^{-3}.

The value of the β parameter, which defines the shape of the potential well, has been fixed to 6 for the out-of-plane configuration and to 7 for the in-plane configurations;[29] x_1 and x_2 are chosen respectively in the range 1.10−1.15 and 1.3−1.75. The values of all parameters, used to generate cuts of the PES's shown in Figure 6, are reported in Tables 4−6.

A routine for the potential energy surfaces for the systems in this paper which provides the full description of rare gas atoms approaching the benzene molecule from any direction is available on request.

References and Notes

(1) Beck, S. M.; Liverman, M. G.; Monts, D. L.; Smalley, R. E. *J. Chem. Phys.* **1979**, *70*, 232−237.
(2) Weber, Th; von Bargen, A.; Riedle, E.; Neusser, H. J. *J. Chem. Phys.* **1990**, *92*, 90−96.
(3) Brupbacher, Th; Bauder, A. *Chem. Phys. Lett.* **1990**, *173*, 435−438.
(4) Weber, Th.; Riedle, E.; Neusser, H. J.; Schlag, E. W. *J. Mol. Struct.* **1991**, *249*, 69−80.
(5) Weber, Th.; Riedle, E.; Neusser, H. J.; Schlag, E. W. *Chem. Phys. Lett.* **1991**, *183*, 77−83.
(6) Fried, L. H.; Mukamel, S. *J. Chem. Phys.* **1992**, *96*, 116−135.
(7) Krause, H.; Neusser, H. J. *J. Chem. Phys.* **1993**, *99*, 6278−6286.
(8) Brupbacher, Th.; Makarewicz, J.; Bauder, A. *J. Chem. Phys.* **1994**, *101*, 9736−9746.
(9) Lenzer, T.; Luther, K. *J. Chem. Phys.* **1996**, *105*, 10944−10953.
(10) Mons, M.; Coutry, A.; Schmidt, M.; Le Calvè, J.; Piuzzi, F.; Dimicoli, I. *J. Chem. Phys.* **1997**, *106*, 1676−1686.
(11) Kim, W.; Felker, P. M. *J. Chem. Phys.* **1997**, *107*, 2193−2204.
(12) Siglow, K.; Neuhauser, R.; Neusser, H. J. *Chem. Phys. Lett.* **1998**, *293*, 19−25.
(13) Neuhauser, R.; Braun, J.; Neusser, H. J.; van den Avoird, A. *J. Chem. Phys.* **1998**, *108*, 8408−8417.
(14) Siglow, K.; Neuhauser, R.; Neusser, H. J. *J. Chem. Phys.* **1999**, *110*, 5589−5599.
(15) Satink, R. G.; Piest, H.; von Helden, G.; Meijer, G. *J. Chem. Phys.* **1999**, *111*, 10 750−10 753.
(16) Bernshtein, V.; Oref, I. *J. Chem. Phys.* **2000**, *112*, 686−697.
(17) Neuhauser, R.; Siglow, K.; Neusser, H. J. *Phys. Rev. Lett.* **1998**, *80*, 5089−5092.
(18) Brandt, R.; Henkel, M.; Pfeil, B.; Seidel, W. *J. Chem. Phys.* **1991**, *95*, 135−140.
(19) Bernstein, R. B.; O'Brien, T. J. P. *Discuss. Faraday Soc.* **1965**, *40*, 35−44.
(20) Pirani, F.; Vecchiocattivi, F. *Mol. Phys.* **1982,** *45*, 1003−1013.
(21) Pirani, F.; Vecchiocattivi, F.; van den Biesen, J. J. H.; van den Meijdenberg, C. J. N. *J. Chem. Phys.* **1981**, *75*, 1042−1043.
(22) Hobza, P.; Bludsky, O.; Selzle, H. L.; Schlag, E. W. *J. Chem. Phys.* **1992**, *97*, 335−340.
(23) Klopper, W.; Lüthi, H. P.; Brupbacher, Th.; Bauder, A. *J. Chem. Phys.* **1994**, *101*, 9747−9754.
(24) Hobza, P.; Selzle, H. L.; Schlag, E. W. *Chem. Rev.* **1994**, *94*, 1767−1785.
(25) Koch, H.; Fernandez, B.; Makarewicz, J. *J. Chem. Phys.* **1999**, *111*, 198−204.
(26) Pirani, F.; Cappelletti, D.; Liuti, G. *Chem. Phys. Lett.* **2001**, *350*, 286.
(27) Cambi, R.; Cappelletti, D.; Pirani, F.; Liuti, G. *J. Chem. Phys.* **1991**, *95*, 1852−1861.
(28) Cappelletti, D.; Liuti, G.; Pirani, F. *Chem. Phys. Lett.* **1991**, *183*, 297−303.
(29) Aquilanti, V.; Cappelletti, D.; Pirani, F. *Chem. Phys* **1996**, *209*, 299−311.
(30) Aquilanti, V.; Cappelletti, D.; Pirani, F. *Chem. Phys. Lett.* **1997**, *271*, 216−222. Aquilanti, V.; Cappelletti, D.; Pirani, F. *J. Chem. Phys.* **1997**, *106*, 5043−5048. Pirani, F.; Giulivi, A.; Cappelletti, D.; Aquilanti, V. *Mol. Phys.* **2000**, *98*, 1749−1762.
(31) Aquilanti, V.; Ascenzi, D.; Braca, E.; Cappelletti, D.; Pirani, F. *Phys. Chem. Chem. Phys.* **2000,** *2*, 4081−4088.
(32) Aquilanti, V.; Ascenzi, D.; Cappelletti, D.; de Castro Vítores, M.; Pirani, F. *J. Chem. Phys.* **1998,** *109*, 3898−3910.
(33) Aquilanti, V.; Ascenzi, D.; Bartolomei, M.; Cappelletti, D.; Cavalli, S.; de Castro Vítores, M.; Pirani, F. *Phys. Rev. Lett.* **1999**, *82*, 69−72.
(34) Aquilanti, V.; Ascenzi, D.; Bartolomei, M.; Cappelletti, D.; Cavalli, S.; de Castro Vítores, M.; Pirani, F. *J. Am. Chem. Soc.* **1999**, *121*, 10 794−10 802.

(35) Pauly, H.; Toennies, J. P. *Methods Exp. Phys.* **1968**, *7A*, 227−341. van den Biesen, J. J. H. In *Atomic and Molecular Beam Methods*; Scoles, G., Ed.; Oxford University Press: New York, 1988; pp 472−498.
(36) Kusch, P. *J. Chem. Phys.* **1964**, *40*, 1−4. von Busch, F. *Z. Physik* **1966**, *193*, 412−425.
(37) Liuti, G.; Luzzatti, E.; Pirani, F.; Volpi, G. G. *Chem. Phys. Lett.* **1987**, *135*, 387−392.
(38) Pirani, F.; Bartolomei, M.; Aquilanti, V.; Cappelletti, D.; Scotoni, M.; Vescovi, M.; Ascenzi, D.; Bassi, D. *Phys. Rev. Lett.* **2001**, *86*, 5035−5038.
(39) Aquilanti, V.; Cappelletti, D.; Lorent, V.; Luzzatti, E.; Pirani, F. *Chem. Phys. Lett.* **1992**, *192*, 153−160.
(40) Hobza, P.; Selzle, H. L.; Schlag, E. W. *J. Am. Chem. Soc.* **1994**, *116*, 3500−3506.
(41) Pirani, F.; Vecchiocattivi, F. *J. Chem. Phys.* **1977**, *66*, 372−373.
(42) Candori, R.; Pirani, F.; Vecchiocattivi, F. *Mol. Phys.* **1983**, *49*, 551−560.
(43) Linse, C. A.; van den Biesen, J. J. H.; van Veen, E. H.; van den Meijdenberg, C. J. N. *Physica* **1979**, *99* A, 166−183.
(44) Reed, K. A.; Warthon, L. *J. Chem. Phys.* **1977**, *66*, 3399−3413.